Reliability Analysis of Inelastic Shell Structures Under Variable Loads

T.N. Trần, P.T. Phạm, Đ.K. Vũ, and M. Staat

Abstract This paper concerns the application of a new algorithm of probabilistic limit and shakedown analysis for shell structures, in which the loading and strength of the material as well as the thickness of the shell are to be considered as random variables. The procedure involves a deterministic limit and shakedown analysis for each probabilistic iteration, which is based on the kinematical approach and the use of the re-parameterized exact Ilyushin yield surface proposed by Burgoyne and Brennan. The limit state function separating the safe and failure regions is defined directly as the difference between the obtained limit load factor and the current load factor. Different kinds of distribution of basic variables are taken into consideration and performed with First- and Second-Order Reliability Methods (FORM/SORM) for calculation of the failure probability of the structure. A non-linear optimization was implemented, which is based on the Sequential Quadratic Programming for finding the design point. Non-linear sensitivity analyses are also performed for computing the Jacobian and the Hessian of

Thanh Ngọc Trần and Phú Tình Phạm
Aachen University of Applied Sciences, Campus Jülich, Institute of Bioengineering, Ginsterweg 1, D-52428 Jülich, Germany; Hanoi Architectural University, Faculty of Civil Engineering, Km 10, Nguyen Trai Road, Thanh Xuan District, Hanoi, Vietnam, e-mail: tran@fh-aachen.de; pham@fh-aachen.de

Đúc Khôi Vũ
Aachen University of Applied Sciences, Campus Jülich, Institute of Bioengineering, Ginsterweg 1, D-52428 Jülich, Germany; University of Erlangen-Nuremberg, Institute of Applied Mechanics, Egerlandstraße 5, D-91058 Erlangen, Germany, e-mail: Vu@ltm.unierlangen.de

Manfred Staat
Aachen University of Applied Sciences, Campus Jülich, Institute of Bioengineering, Ginsterweg 1, D-52428 Jülich, Germany, e-mail: m.staat@fh-aachen.de

D. Weichert, A. Ponter (eds.), *Limit States of Materials and Structures*,
DOI 10.1007/978-1-4020-9634-1_7,

the limit state function. This direct approach reduces considerably the necessary knowledge of uncertain technological input data, computing costs and the numerical error. Numerical examples are presented to show the validity and effectiveness of the present method.

1 Introduction

The integrity assessment of pressure vessels and piping by means of direct plasticity methods has been a problem of great interest to many designers, especially in the design of industrial and nuclear power plants. The new European pressure vessel standard EN 13445-3 is based on perfectly plastic limit and shakedown analysis (LISA) [8] thus indicating the industrial need for LISA software for safe and reliable design of such structures. Additionally, practical design codes often prescribe what kind of values to choose for safety factor of the resistance and of the loads for a given problem since all resistance and loading variables are generally random. To this case, structural reliability-based LISA can be performed to establish a rational basis for the choice of safety factors. Probabilistic limit analysis has been proposed earlier for frames using linear programming [2, 15].

The present paper concerns the application of a new upper bound algorithm of probabilistic limit and shakedown analysis for shell structures with the help of the finite element method. Both deterministic and probabilistic limit and shakedown analyses are presented. For the deterministic problem, three failure modes of structure such as plastic collapse, alternating plasticity (low cycle fatigue, LCF) and ratchetting are analyzed based on the upper bound approach. This direct method leads to convex minimum problems which results in a failure mechanism with a unique limit load or shakedown load.

Probabilistic limit and shakedown analysis deals with uncertainties originating from the loads, material strength and thickness of the shell. Based on a direct definition of the limit state function, the calculation of the failure probability may be efficiently solved by using the First- and Second-Order Reliability Methods (FORM/SORM) which are based on the computation of the most probable failure point, the so-called design point. Since the deterministic analysis is a sub-routine of the probabilistic one, even a small error in the deterministic model can lead to a big error in the reliability analysis because of the sensitivity of the failure probability. Due to this reason, a yield criterion which is exact for rigid-perfectly plastic material behaviour and is expressed in terms of stress resultants, namely the exact Ilyushin yield surface, will be applied instead of the simplified Ilyushin yield surface (linear or quadratic approximations). Along similar lines the lower bound probabilistic LISA has been developed for volume elements in a series of papers by Heitzer and Staat [11, 12, 18].

Although the deterministic LISA subproblem has a unique solution it is well known that all possible failure mechanisms contribute to the failure probability [2, 16]. The kinematic or upper bound method may give the exact failure probability only if all mechanisms are considered. In practice often few dominant mechanisms can give reasonable results. In [21] a bulge method proposed in [14] has been applied to the reliability problems of shells which constructs "barriers" around previously found (FORM/SORM) solutions, thus forcing the algorithm to seek a new solution. In this way the complete reliability problem may be solved. For the linear optimization formulation of the static or lower bound approach a different method has been suggested in [4] and extended in [1] for plane frame structures. Here we restrict the presentation to the calculation of the mechanism with the highest probability only.

2 Plastic Dissipation Function in Terms of Strain Resultants

For our purpose of dealing with the reliability problem, the loads, the yield limit σ_y and the thickness h of the shell are considered as random variables. The yield limit can be modeled as stochastic field and discretized through a vector $\mathbf{Y} = [Y_1, Y_2, \ldots, Y_m]^T$ of random variables Y_i at the ith Gaussian point so that $\tilde{\boldsymbol{\sigma}}_y = \mathbf{Y}\sigma_y$. Assuming the yield stress as a random field could render the whole procedure very burdensome. The yield stress can be modeled as a stochastic variable $\sigma_y = Y\sigma_0$ if the Y_i are fully correlated. For simplicity we restrict ourselves to this case with homogeneous material, and shells of constant thickness h. So we can always write

$$\sigma_y = Y\sigma_0, \quad h = Zh_0, \tag{1}$$

where σ_0, h_0 are constant reference values and Y, Z are random variables. Only for the simplicity of the presentation it is assumed that all parts of the shell structure are made from the same material. The software implementation has been made without this restriction.

It is convenient to define the non-dimensional "engineering" stress and strain resultant vectors as follows

$$\tilde{\boldsymbol{\sigma}} = [\boldsymbol{n}\ \boldsymbol{m}]^T, \quad \tilde{\boldsymbol{\varepsilon}} = [\bar{\boldsymbol{e}} \quad \boldsymbol{k}]^T, \tag{2}$$

where

$$\begin{aligned} \boldsymbol{n} &= \frac{1}{N_0}\,[N_{11} \quad N_{22} \quad N_{12}]^T, \quad \boldsymbol{m} = \frac{1}{M_0}\,[M_{11} \quad M_{22} \quad M_{12}]^T, \\ \bar{\boldsymbol{e}} &= \frac{1}{\varepsilon_0}\,[\bar{\varepsilon}_{11} \quad \bar{\varepsilon}_{22} \quad 2\bar{\varepsilon}_{12}]^T, \quad \boldsymbol{k} = \frac{1}{\kappa_0}\,[\kappa_{11} \quad \kappa_{22} \quad 2\kappa_{12}]^T, \end{aligned} \tag{3}$$

and $N_0 = \sigma_0 h_0$, $M_0 = \sigma_0 h_0^2/4$, $\varepsilon_0 = \sigma_0(1-\nu^2)/E$ and $\kappa_0 = 4\varepsilon_0/h_0$ are the normalized quantities. In that way the quadratic strain intensities can be defined by

$$\begin{aligned} P_\varepsilon &= \frac{3}{4}\left(\mathrm{d}\tilde{\boldsymbol{\varepsilon}}^p\right)^T \mathbf{P}_1 \mathrm{d}\tilde{\boldsymbol{\varepsilon}}^p \qquad (\geq 0), \\ P_{\varepsilon\kappa} &= 3\left(\mathrm{d}\tilde{\boldsymbol{\varepsilon}}^p\right)^T \mathbf{P}_2 \mathrm{d}\tilde{\boldsymbol{\varepsilon}}^p, \\ P_\kappa &= 12\left(\mathrm{d}\tilde{\boldsymbol{\varepsilon}}^p\right)^T \mathbf{P}_3 \mathrm{d}\tilde{\boldsymbol{\varepsilon}}^p \qquad (\geq 0). \end{aligned} \tag{4}$$

where $\mathrm{d}\tilde{\boldsymbol{\varepsilon}}^p$ denotes the plastic strain increment resultant vector, $\mathbf{P}$ and its inverse $\mathbf{P}^{-1}$, $\mathbf{P}_i (i = 1, 2, 3)$ are

$$\begin{aligned} &\mathbf{P} = \begin{pmatrix} 1 & -1/2 & 0 \\ -1/2 & 1 & 0 \\ 0 & 0 & 3 \end{pmatrix}, \quad \mathbf{P}^{-1} = \begin{pmatrix} 4/3 & 2/3 & 0 \\ 2/3 & 4/3 & 0 \\ 0 & 0 & 1/3 \end{pmatrix}, \\ &\mathbf{P}_1 = \begin{pmatrix} \mathbf{P}^{-1} & \mathbf{0} \\ \mathbf{0} & \mathbf{0} \end{pmatrix}, \quad \mathbf{P}_2 = \begin{pmatrix} \mathbf{0} & \mathbf{P}^{-1}/2 \\ \mathbf{P}^{-1}/2 & \mathbf{0} \end{pmatrix}, \quad \mathbf{P}_3 = \begin{pmatrix} \mathbf{0} & \mathbf{0} \\ \mathbf{0} & \mathbf{P}^{-1} \end{pmatrix}. \end{aligned} \tag{5}$$

Ilyushin [13] derived an exact form of the yield surface in terms of the stress resultant for a linear elastic-perfectly plastic isotropic material which obeys the von Mises criterion. A simpler form of this yield surface (though still exact) was proposed by Burgoyne and Brennan [3] by introducing the parameters

$$\upsilon = \frac{P_\varepsilon}{P_\kappa}, \beta = -\frac{P_{\varepsilon\kappa}}{P_\kappa} \quad \text{and} \quad \gamma = \upsilon - \beta^2, \tag{6}$$

where β and γ are proposed as two independent parameters for the description of the yield surface. With these parameters, the plastic dissipation function for a shell structure may be written in the form [20, 21]

$$D^p(\dot{\tilde{\boldsymbol{\varepsilon}}}) = Y N_0 \varepsilon_0 \sqrt{\frac{P_\kappa}{3}} \left(\beta_1 \sqrt{\beta_1^2 + \gamma} + \beta_2 \sqrt{\beta_2^2 + \gamma} + \gamma K_0 \right), \tag{7}$$

where β_1, β_2 and K_0 are

$$\beta_1 = \frac{Z}{2} - \beta, \quad \beta_2 = \frac{Z}{2} + \beta, \quad K_0 = \ln\left(\frac{\sqrt{\beta_1^2 + \gamma} + \beta_1}{\sqrt{\beta_2^2 + \gamma} - \beta_2} \right). \tag{8}$$

It should be noted here, that the value of K_0 will become indefinite if both conditions $|\beta| \leq 0.5Z$ and $\gamma = 0$ are fulfilled. However, as long as γ is not exactly equal to zero, but assumes to some small positive number, a "regularized" evaluation of K_0 may be obtained [17]. Otherwise, in general, D^p is convex [5] but not everywhere differentiable as shown for continuum problems. It is only differentiable in the plastified region of the structure, i.e. $P_\kappa > 0$. In order to allow a direct non-linear, non-smooth, constrained

optimization problem, a "smooth regularization method" should be used to overcome the non-differentiability of the objective function as will be discussed in the following section.

3 Deterministic Limit and Shakedown Algorithm

Consider a convex polyhedral load domain $\mathcal{L}$ and a special loading path consisting of all load vertices $\hat{P}_k$ $(k = 1, \ldots, m)$ of $\mathcal{L}$. Let the fictitious elastic generalized stress vector be denoted by $\boldsymbol{\sigma}$. By discretizing the whole structure with the help of finite elements and the application of Koiter's theorem, the shakedown limit $\alpha_{\lim}$, which is the smaller one of the low cycle fatigue limit and the ratchetting limit, may be found by the following minimization

$$\alpha_{\lim} = \min \sum_{i=1}^{NG} \sum_{k=1}^{m} w_i Y N_0 \varepsilon_0 \sqrt{\frac{P_\kappa}{3}} \left(\beta_1 \sqrt{\beta_1^2 + \gamma} + \beta_2 \sqrt{\beta_2^2 + \gamma} + \gamma K_0 \right),$$

$$\text{s.t.} : \begin{cases} \sum\limits_{k=1}^{m} \dot{\tilde{\varepsilon}}_{ik} = \mathbf{B}_i \dot{\boldsymbol{u}} & \forall i = 1, \ldots, NG, \\ \sum\limits_{i=1}^{NG} \sum\limits_{k=1}^{m} w_i N_0 \boldsymbol{\varepsilon}_0 \dot{\tilde{\boldsymbol{\varepsilon}}}_{ik}^T \tilde{\boldsymbol{\sigma}}_{ik}^E = 1, \end{cases} \tag{9}$$

in which $\dot{\boldsymbol{u}}$ denotes the velocity fields, $\mathbf{B}_i$ denotes the deformation matrix, and w_i is the weighting factor of the i^{th} Gauss point $(i = 1, \ldots, NG)$. For the sake of simplicity some new notations are introduced

$$\dot{\mathrm{e}}_{ik} = w_i \dot{\tilde{\boldsymbol{\varepsilon}}}_{ik}, \quad \mathrm{t}_{ik} = N_0 \varepsilon_0 \tilde{\boldsymbol{\sigma}}_{ik}^E, \quad \hat{\mathbf{B}}_i = w_i \mathbf{B}_i, \tag{10}$$

where $\dot{\mathrm{e}}_{ik}, \mathrm{t}_{ik}, \hat{\mathbf{B}}_i$ are the new strain rate vector, the new fictitious elastic stress vector and the new deformation matrix, respectively. By substituting (10) into (9) we obtain a simplified version for the upper bound shakedown analysis

$$\alpha_{\lim} = \min \sum_{i=1}^{NG} \sum_{k=1}^{m} Y N_0 \varepsilon_0 \sqrt{\frac{P_\kappa}{3}} \left(\beta_1 \sqrt{\beta_1^2 + \gamma} + \beta_2 \sqrt{\beta_2^2 + \gamma} + \gamma K_0 \right),$$

$$\text{s.t.} : \begin{cases} \sum\limits_{k=1}^{m} \dot{\mathrm{e}}_{ik} = \hat{\mathbf{B}}_i \dot{\boldsymbol{u}} & \forall i = 1, \ldots, NG, \\ \sum\limits_{i=1}^{NG} \sum\limits_{k=1}^{m} \dot{\mathrm{e}}_{ik}^T \mathrm{t}_{ik} = 1. \end{cases} \tag{11}$$

To eliminate the first optimization constraint a penalty method is used. To this purpose, let us write the penalty function as

$$F_P = \sum_{i=1}^{NG} \left\{ \begin{array}{l} \sum\limits_{k=1}^{m} \left(Y N_0 \varepsilon_0 \sqrt{\frac{P_\kappa}{3}} \left(\beta_1 \sqrt{\beta_1^2 + \gamma} + \beta_2 \sqrt{\beta_2^2 + \gamma} + \gamma K_0 \right) \right) \\ + \frac{c}{2} \left(\sum\limits_{k=1}^{m} \dot{\mathrm{e}}_{ik} - \hat{\mathbf{B}}_i \dot{\boldsymbol{u}} \right)^T \left(\sum\limits_{k=1}^{m} \dot{\mathrm{e}}_{ik} - \hat{\mathbf{B}}_i \dot{\boldsymbol{u}} \right) \end{array} \right\} \tag{12}$$

$$= \sum_{i=1}^{NG} \left\{ \sum_{k=1}^{m} (Y \eta_{ik}) + \frac{c}{2} \left(\sum_{k=1}^{m} \dot{\mathbf{e}}_{ik} - \hat{\mathbf{B}}_i \dot{\boldsymbol{u}} \right)^T \left(\sum_{k=1}^{m} \dot{\mathrm{e}}_{ik} - \hat{\mathbf{B}}_i \dot{\boldsymbol{u}} \right) \right\},$$

where c is a penalty parameter such that $c \gg 1$. For the sake of simplicity, the same value of c is assumed at every Gauss point of the structure. The second constraint can be eliminated by using the dual Lagrange function

$$F_{PL} = F_P - \lambda \left(\sum_{i=1}^{NG} \sum_{k=1}^{m} \dot{\mathrm{e}}_{ik}^T \mathrm{t}_{ik} - 1 \right), \tag{13}$$

where λ is the Lagrange multiplier. The major numerical obstacle appears here due to the non-differentiability of the objective function F_{PL} and the singularity of K_0 as discussed in Sect. 2. A regularization method can be used here by replacing the original plastic dissipation function $D^p(\dot{\boldsymbol{\varepsilon}}^p)$ by its disturbed one $D^p(\dot{\boldsymbol{\varepsilon}}^p, \eta_0^2)$. In the new plastic dissipation function $D^p(\dot{\boldsymbol{\varepsilon}}^p, \eta_0^2)$, η_0^2 is a small positive number which is added to γ and P_κ, i.e. $\gamma \to \gamma + \eta_0^2$ and $P_\kappa \to P_\kappa + \eta_0^2$. In this way, all elements in the structure are seen as plastified or on the plastified verge.

By applying Newton's method to solve the KKT conditions of Eq. (13) we obtain the Newton directions $\mathrm{d}\dot{\boldsymbol{u}}$ and $\mathrm{d}\dot{\tilde{\boldsymbol{\varepsilon}}}_{ik}$, which assure that a suitable step along them will lead to a decrease of the objective function $\alpha_{\lim}$. If the relative improvement between two steps is smaller than a given constant, the algorithm stops and leads to the shakedown limit factor. Details of the iterative algorithm can be found in [20, 21].

4 Probabilistic Limit and Shakedown Algorithm

Denote by $\mathbf{X} = (X_1, X_1, \ldots, X_n)$ an n-dimensional random vector characterizing uncertainties in the structure and load parameters. The limit state function $g(\mathbf{x}) = 0$, which is based on the comparison of a structural resistance (threshold) and loading, defines the limit state hyper-surface ∂F which separates the failure region $F = \{\, \mathbf{x} |\, g(\mathbf{x}) < 0 \}$ from the safe region. The failure probability P_f is the probability that $g(\mathbf{X})$ is non-positive, i.e.

$$P_f = P\left(g(\mathbf{X}) \le 0\right) = \int_F f_X(\mathbf{x}) \mathrm{d}x, \tag{14}$$

where $f_X(\mathbf{x})$ is the n-dimensional joint probability density function. Usually, it is not possible to calculate P_f analytically since the form of the limit state surface is very complex. For the general cases, there are several approximate methods to compute the failure probability P_f. Direct Monte Carlo Simulation (MCS) becomes increasingly expensive with the increase of the structural reliability. Acceptable failure probabilities might be in the range of 10^{-4} to 10^{-6}. They are even much lower in nuclear reactor technology. For a validation that the failure probability P_f is less than an accepted limit P_c, the sample size required for direct (MCS) must be at least $100/P_c$ leading to a minimum sample size in the range of 10^6 to 10^8. Such a large number exceeds particularly for complex FE-models available resources by far. The numerical effort can be reduced considerably by variance reduction methods like Importance Sampling and by Response Surface Methods (RSM). However, the most effective analysis is based on First- and Second-Order Reliability Methods (FROM/SORM) if gradient information is available [9].

4.1 First- and Second-Order Reliability Methods

(FROM/SORM) (alternatively referred as the most likely failure point method) is used here to perform uncertainty analysis. Practical experience with (FROM/SORM)algorithms indicates that their estimates usually provide satisfactory reliability measures. Especially in the case of small failure probability (large reliability), (FROM/SORM) are extremely efficient compared with the (MCS) method regarding the requirement of computer time, such as the Central Processing Unit (CPU). In (FROM/SORM) the probability of failure is computed in three steps. Firstly the physical space $\mathbf{x}$ of uncertain parameters, $\mathbf{X}$, is transformed into a new n-dimensional space, $\mathbf{u}$, consisting of independent standard Gaussian variables $\mathbf{U}$. By this transformation, the original limit state $g(\mathbf{x}) = 0$ is mapped into the new limit state $g(\mathbf{u}) = 0$ in the $\mathbf{u}$ space. Secondly the design point or β_{HL}-point is determined by an appropriate non-linear optimization algorithm. This is the point on the limit state surface having the shortest distance to the origin in the $\mathbf{u}$ space. Due to the rotational symmetry and exponential decay of the probability density, the design point has the highest probability among all points in the failure domain. It follows that the neighbourhood of this point makes the dominant contribution to the failure probability. Details of the non-linear optimization algorithm for finding the design point which is based on the sequential quadratic programming (SQP) can be found in [20,21]. Thirdly the limit state surface $g(\mathbf{u}) = 0$ is approximated by a tangential hypersurface at the design point. This corresponds to an approximating hyperplane $g_L(\mathbf{u}) = 0$ (linear or first-order) and hyperparaboloid $g_Q(\mathbf{u}) = 0$ (quadratic or second-order), respectively (see Fig. 1). The failure probability P_f is thus approximated by $P_{f,L} = P\left(g_L\left(\mathbf{u}\right) < 0\right)$ in FORM

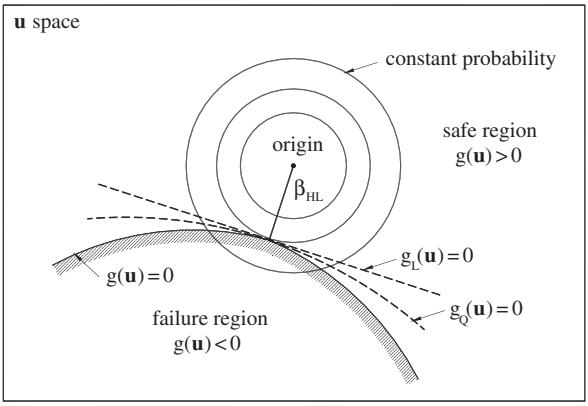

Fig. 1 Safe and failure regions based on linear and quadratic approximations in **u** space

$$P_{f,L} = \Phi(-\beta_{HL}) = \frac{1}{\sqrt{2\pi}} \int_{-\infty}^{-\beta_{HL}} e^{-0.5z^2} \mathrm{d}z, \tag{15}$$

and by $P_{f,Q} = P\left(g_Q\left(\mathbf{u}\right) < 0\right)$ in SORM [10, 22]

$$P_{f,Q} = S_1 + S_2 + S_3, \tag{16}$$

with

$$S_1 = \Phi\left(-\beta_{HL}\right) \prod_{j=1}^{n-1} \left(1 - \beta_{HL}\kappa_j\right)^{-1/2},$$

$$S_2 = \left[\beta_{HL}\Phi\left(-\beta_{HL}\right) - \phi\left(\beta_{HL}\right)\right] \left\{ \prod_{j=1}^{n-1} \left(1 - \beta_{HL}\kappa_j\right)^{-1/2} - \prod_{j=1}^{n-1} \left(1 - \left(\beta_{HL} + 1\right)\kappa_j\right)^{-1/2} \right\},$$

$$S_3 = \left(\beta_{HL} + 1\right) \left[\beta_{HL}\Phi\left(-\beta_{HL}\right) - \phi\left(\beta_{HL}\right)\right] \times \left\{ \prod_{j=1}^{n-1} \left(1 - \beta_{HL}\kappa_j\right)^{-1/2} - \mathrm{Re}\left[\prod_{j=1}^{n-1} \left(1 - \left(\beta_{HL} + i\right)\kappa_j\right)^{-1/2} \right] \right\},$$

with κ_j are $n-1$ principle curvatures at the design point. The calculation of κ_j normally needs the second derivatives of the limit state function.

4.2 Definition of the Limit State Function

The shakedown load factor $\alpha_{\lim}$ which is calculated by the constraint minimum problem (11) defines the ratio between the shakedown load $P_{\lim}$ and actual load P of the structure, i.e.

$$\alpha_{\lim} = \frac{P_{\lim}}{P}. \tag{17}$$

As mentioned above, the limit state function contains the parameters of structural resistance and loading. Thus it can be defined as $g = P_{\lim} - P = P(\alpha_{\lim} - 1)$. For the sake of simplicity, the limit state function g can be normalized with the actual load P and then becomes

$$g = \alpha_{\lim} - 1. \tag{18}$$

It can be seen that the limit state function is a function of the load, the random variables yield stress and thickness. The actual load P is defined in n components by using the concept of a constant reference load P^0 as follows

$$\begin{aligned} P^0 &= P_1^0 + P_2^0 + \ldots + P_n^0, \\ P &= x_1 P_1^0 + x_2 P_2^0 + \ldots + x_n P_n^0, \end{aligned} \tag{19}$$

where x_j is the realization of the j^{th} basic load variable X_j $(j = 1, n)$. The corresponding actual fictitious elastic stress fields $\tilde{\boldsymbol{\sigma}}^E$ can also be described in the same way

$$\tilde{\boldsymbol{\sigma}}^E = x_1 \tilde{\boldsymbol{\sigma}}_1^0 + x_2 \tilde{\boldsymbol{\sigma}}_2^0 + \ldots + x_n \tilde{\boldsymbol{\sigma}}_n^0. \tag{20}$$

From (19) and (20), the corresponding normalized fictitious elastic stress fields $\mathbf{t}$ are obtained

$$\mathbf{t} = N_0 \varepsilon_0 \tilde{\boldsymbol{\sigma}} = N_0 \varepsilon_0 \left[x_1 \tilde{\boldsymbol{\sigma}}_1^0 + x_2 \tilde{\boldsymbol{\sigma}}_2^0 + \ldots + x_n \tilde{\boldsymbol{\sigma}}_n^0 \right] = x_1 \mathbf{t}_1 + x_2 \mathbf{t}_2 + \ldots + x_n \mathbf{t}_n. \tag{21}$$

4.3 Sensitivity Analyses

The sensitivity analyses provide the Jacobian and the Hessian of the limit state function, $\partial g / \partial \mathbf{x}$ and $\partial^2 g / \partial \mathbf{x}^2$, which are needed for the SQP, FORM and SORM algorithms. They also provide a quantitative measure of the first- and second-order change in the optimal value function or show how the solution is affected by changes in the problem data. The necessary data for the

calculation of the Jacobian and the Hessian are available after the execution of the deterministic shakedown analysis since they are based on the limit load factor $\alpha_{\lim}$.

In order to get the sensitivity of the limit state function g in the physical space $\mathbf{x}$, one requirement from Eq. (18) is that the derivatives of the limit load factor $\alpha_{\lim}$ must be available. Let $(\dot{\mathbf{e}}^*_{ik}, \mathbf{u}^*, \lambda^*)$ be the solutions of the optimization problem (11). At the optimal point, the first derivative of the limit load factor $\alpha_{\lim}$ versus the j^{th} load variable X_j and the yield stress variable Y can be calculated as follows [20, 21]

$$\frac{\partial \alpha_{\lim}}{\partial X_j} = \left.\frac{\partial F_{PL}}{\partial X_j}\right|_{\left(\dot{\mathbf{e}}^*_{ik}, \mathbf{u}^*, \lambda^*\right)} = -\lambda \sum_{i=1}^{NG}\sum_{k=1}^{m} \dot{\mathrm{e}}^T_{ik} \left.\frac{\partial \mathrm{t}_{ik}}{\partial X_j}\right|_{\left(\dot{\mathbf{e}}^*_{ik}, \lambda^*\right)}$$

$$= -\lambda \sum_{i=1}^{NG}\sum_{k=1}^{m} \dot{\mathrm{e}}^T_{ik} \mathrm{t}_{ik,j}\Big|_{\left(\dot{\mathbf{e}}^*_{ik}, \lambda^*\right)}, \tag{22}$$

$$\frac{\partial \alpha_{\lim}}{\partial Y} = \left.\frac{\partial F_{PL}}{\partial Y}\right|_{\left(\dot{\mathbf{e}}^*_{ik}, \mathbf{u}^*, \lambda^*\right)} = \left.\frac{\partial}{\partial Y}\left(\sum_{i=1}^{NG}\sum_{k=1}^{m} Y \eta_{ik}\right)\right|_{\left(\dot{\mathbf{e}}^*_{ik}\right)}$$

$$= \sum_{i=1}^{NG}\sum_{k=1}^{m} \eta^*_{ik} = \frac{\alpha_{\lim}}{Y}. \tag{23}$$

The derivatives of the limit load factor $\alpha_{\lim}$ versus the random thickness variable Z can be determined in the same way assuming the form

$$\frac{\partial \alpha_{\lim}}{\partial Z} = \left.\frac{\partial F_{PL}}{\partial Z}\right|_{\left(\dot{\mathbf{e}}^*_{ik}, \mathbf{u}^*, \lambda^*\right)}$$

$$= \left.\frac{\partial}{\partial Z}\left(\sum_{i=1}^{NG}\sum_{k=1}^{m}\left(Y N_0 \varepsilon_0 \sqrt{\frac{P_k}{3}}\left(\beta_1\sqrt{\beta_1^2+\gamma} + \beta_2\sqrt{\beta_2^2+\gamma} + \gamma K_0\right)\right)\right)\right|_{\dot{\mathbf{e}}^*_{ik}}$$

$$= \left.\sum_{i=1}^{NG}\sum_{k=1}^{m}\left(Y N_0 \varepsilon_0 \sqrt{\frac{P_k}{3}}\left(\sqrt{\beta_1^2+\gamma} + \sqrt{\beta_2^2+\gamma}\right)\right)\right|_{\dot{\mathbf{e}}^*_{ik}}. \tag{24}$$

The second partial derivatives of the limit state function versus the j^{th} load variable X_j and the yield stress variable Y can be obtained directly from an analytical derivation of the first derivatives [20, 21]

$$\frac{\partial^2 \alpha_{\lim}}{\partial X_l X_j} = \frac{\partial}{\partial X_l}\left(-\lambda \sum_{i=1}^{NG}\sum_{k=1}^{m} \dot{\mathrm{e}}_{ik}^T \mathrm{t}_{ik,j}\right)\Bigg|_{(\dot{\boldsymbol{\varepsilon}}_{ik}^*,\lambda^*)}$$

$$= -\frac{\partial \lambda}{\partial X_l}\sum_{i=1}^{NG}\sum_{k=1}^{m} \dot{\mathrm{e}}_{ik}^T \mathrm{t}_{ik,j}\Bigg|_{(\dot{\boldsymbol{\varepsilon}}_{ik}^*,\lambda^*)} - \lambda \sum_{i=1}^{NG}\sum_{k=1}^{m} \mathrm{t}_{ik,j}^T \frac{\partial \dot{\mathrm{e}}_{ik}}{\partial X_l}\Bigg|_{(\dot{\boldsymbol{\varepsilon}}_{ik}^*,\lambda^*)}, \tag{25}$$

$$\frac{\partial^2 \alpha_{\lim}}{\partial Y^2} = \frac{\partial}{\partial Y}\left(\frac{\alpha_{\lim}}{Y}\right)\Bigg|_{\dot{\boldsymbol{\varepsilon}}_{ik}^*} = \left(\frac{1}{Y}\frac{\partial \alpha_{\lim}}{\partial Y} - \frac{\alpha_{\lim}}{Y^2}\right)\Bigg|_{\dot{\boldsymbol{\varepsilon}}_{ik}^*} = \left(\frac{1}{Y}\frac{\alpha_{\lim}}{Y} - \frac{\alpha_{\lim}}{Y^2}\right)\Bigg|_{\dot{\boldsymbol{\varepsilon}}_{ik}^*} = 0, \tag{26}$$

where

$$\frac{\partial \dot{\mathrm{e}}_{ik}}{\partial X_l} = \mathrm{G}_{ik}^{-1}\mathrm{t}_{ik}\frac{\partial \lambda}{\partial X_l} + \lambda \mathrm{G}_{ik}^{-1}\mathrm{t}_{ik,l}, \quad \frac{\partial \lambda}{\partial X_l} = \frac{\dfrac{1}{\lambda}\dfrac{\partial \alpha_{\lim}}{\partial X_l} - \lambda \sum\limits_{i=1}^{NG}\sum\limits_{k=1}^{m} \mathrm{t}_{ik}^T \mathrm{G}_{ik}^{-1}\mathrm{t}_{ik,l}}{\sum\limits_{i=1}^{NG}\sum\limits_{k=1}^{m} \mathrm{t}_{ik}^T \mathrm{G}_{ik}^{-1}\mathrm{t}_{ik}}, \tag{27}$$

with $\mathrm{G}_{ik} = \partial^2 F_{PL}/\partial \dot{\mathrm{e}}_{ik}^2$. It can be seen from (26) that the limit state function is a linear function of the yield stress variable Y. In the case of a heterogeneous material, we will obtain at different Gaussian points i eventually different yield stress variables Y_i. Then the limit state function is no more a linear function of these variables.

The second derivatives of $\alpha_{\lim}$ versus the thickness variable Z are obtained by taking the derivatives of Eqs. (22), (23) and (24), versus Z, which gives

$$\frac{\partial^2 \alpha_{\lim}}{\partial X_j \partial Z} = -\frac{\partial \lambda}{\partial Z}\sum_{i=1}^{NG}\sum_{k=1}^{m} \dot{\mathrm{e}}_{ik}^T \mathrm{t}_{ik,j}\Bigg|_{(\dot{\boldsymbol{\varepsilon}}_{ik}^*,\lambda^*)} - \lambda \sum_{i=1}^{NG}\sum_{k=1}^{m} \mathrm{t}_{ik,j}^T \frac{\partial \dot{\mathrm{e}}_{ik}}{\partial Z}\Bigg|_{(\dot{\boldsymbol{\varepsilon}}_{ik}^*,\lambda^*)}, \tag{28}$$

$$\frac{\partial^2 \alpha_{\lim}}{\partial Y \partial Z} = \sum_{i=1}^{NG}\sum_{k=1}^{m}\left(N_0 \varepsilon_0 \sqrt{\frac{P_k}{3}}\left(\sqrt{\beta_1^2+\gamma}+\sqrt{\beta_2^2+\gamma}\right)\right)\Bigg|_{\dot{\boldsymbol{\varepsilon}}_{ik}^*}, \tag{29}$$

$$\frac{\partial^2 \alpha_{\lim}}{\partial Z^2} = \left\{\begin{array}{l} \sum\limits_{i=1}^{NG}\sum\limits_{k=1}^{m} \dfrac{\sqrt{3}}{4\sqrt{P_k}} Y N_0 \varepsilon_0 \left(\dfrac{\partial \dot{\mathbf{e}}_{ik}}{\partial Z}\right)^T \times \\ \left\{\begin{array}{l} 16\left(\sqrt{\beta_1^2+\gamma}+\sqrt{\beta_2^2+\gamma}\right)\mathbf{P}_3 + 8\left(\dfrac{\beta_1}{\sqrt{\beta_1^2+\gamma}} - \dfrac{\beta_2}{\sqrt{\beta_2^2+\gamma}}\right)\mathsf{A} \\ + \left(\dfrac{1}{\sqrt{\beta_1^2+\gamma}} + \dfrac{1}{\sqrt{\beta_2^2+\gamma}}\right)\mathsf{B} \end{array}\right\}\dot{\mathbf{e}}_{ik} \end{array}\right\}\Bigg|_{\dot{\boldsymbol{\varepsilon}}_{ik}^*} \tag{30}$$

$$+ \sum_{i=1}^{NG}\sum_{k=1}^{m}\left(Y N_0 \varepsilon_0 \sqrt{\frac{P_k}{3}}\left(\frac{\beta_1}{2\sqrt{\beta_1^2+\gamma}} + \frac{\beta_2}{2\sqrt{\beta_2^2+\gamma}}\right)\right)\Bigg|_{\dot{\boldsymbol{\varepsilon}}_{ik}^*},$$

where

$$\begin{aligned} \mathsf{A} &= \mathbf{P}_2 + 4\beta\mathbf{P}_3, \\ \mathsf{B} &= \mathbf{P}_1 + 8\beta\mathbf{P}_2 - 16\left(\gamma - \beta^2\right)\mathbf{P}_3. \end{aligned} \tag{31}$$

The derivatives of λ and $\dot{\mathrm{e}}_{ik}$ versus Z are obtained in the following way. Firstly differentiate the Lagrange function F_{PL} in Eq. (13) versus $\dot{\mathbf{e}}_{ik}$, then taking derivatives of the obtained result $\partial^2 F_{PL}/\partial\dot{\mathbf{e}}_{ik}$ versus Z and using the chain rule for two variables $\dot{\mathrm{e}}_{ik}, \lambda$. After some manipulations one has

$$\frac{\partial\dot{\mathrm{e}}_{ik}}{\partial Z} = \mathrm{G}_{ik}^{-1}\mathrm{t}_{ik}\frac{\partial\lambda}{\partial Z} - \frac{1}{\sqrt{\hat{P}_\kappa}}\mathrm{G}_{ik}^{-1}\frac{\partial\mathrm{H}_{ik}}{\partial Z}\dot{\mathrm{e}}_{ik}, \tag{32}$$

$$\frac{\partial\lambda}{\partial Z} = \frac{\sum\limits_{i=1}^{NG}\sum\limits_{k=1}^{m}\dfrac{1}{\sqrt{\hat{P}_\kappa}}\mathrm{t}_{ik}^T\mathrm{G}_{ik}^{-1}\dfrac{\partial\mathrm{H}_{ik}}{\partial Z}\dot{\mathrm{e}}_{ik}}{\sum\limits_{i=1}^{NG}\sum\limits_{k=1}^{m}\mathrm{t}_{ik}^T\mathrm{G}_{ik}^{-1}\mathrm{t}_{ik}}, \tag{33}$$

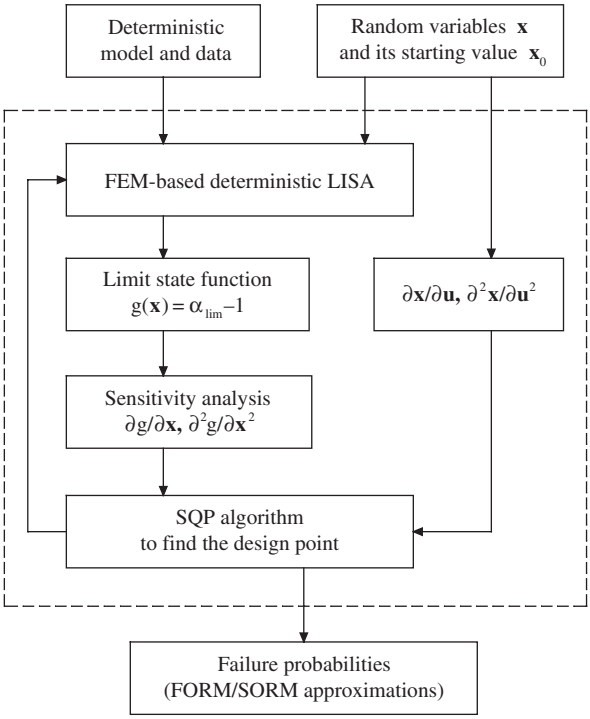

Fig. 2 Flowchart of the probabilistic limit and shakedown analysis

with

$$\frac{\partial H_{ik}}{\partial Z} = Y\tilde{N}_0\tilde{\varepsilon}_0 \begin{pmatrix} 4\sqrt{3}\left(\sqrt{\beta_1^2+\gamma}+\sqrt{\beta_2^2+\gamma}\right)\mathbf{P}_3 \\ +2\sqrt{3}\left(\frac{\beta_1}{\sqrt{\beta_1^2+\gamma}}-\frac{\beta_2}{\sqrt{\beta_2^2+\gamma}}\right)\mathsf{A} \\ +\frac{\sqrt{3}}{4}\left(\frac{1}{\sqrt{\beta_1^2+\gamma}}+\frac{1}{\sqrt{\beta_2^2+\gamma}}\right)\mathsf{B} \end{pmatrix}. \tag{34}$$

The flowchart in Fig. 2 contains the logical connections of the main analysis steps as they have been implemented. In each probabilistic iteration, i.e. the iteration for finding the design point, two deterministic loops are required, the first one provides information for sensitivity analysis and the second one for the simple line search algorithm.

5 Numerical Examples

The probabilistic limit and shakedown algorithm described above is programmed and implemented in the finite element package Code_Aster 7.3 [6]. The 4-noded quadrangular isoparametric flat shell element, the DKT element, which is based on Kirchhoff's hypothesis, was applied. Higher order shell elements are not available in Code_Aster. In all numerical examples, the structures are made of elastic-perfectly plastic material. For each test case, some existing analytical and numerical solutions found in literature are briefly represented and compared. The finite element discretizations were realized by the personal pre- and post-processor GiD 7.2 [8].

Here only the most probable failure mode is calculated with FORM/SORM in all examples. Excluding failure modes one after the other by a barrier from the further search in FORM/SORM it was possible to identify the contribution of multiple failure modes of a plane frame and obtain better approximations of the failure probability [21]. In this test case taken from [16] the yield stress has only been assumed as mutually independent random variable with different log-normal distributions for the different beams in the frame. Before publication the proposed method may need further testing with more complex examples.

5.1 Pipe Bend Under In-Plane Bending Moment

The pipe bends have been a problem of great interest to many designers. They have a complex response to bending moments. When an external moment is applied to one end of the pipe bend, the annular cross section tends to deform significantly both in and out of its own plane, i.e. it is subjected to warping and ovalization. Due to their curved geometry, the pipe bends are very flexible and forced to accommodate large displacements resulting in larger stresses

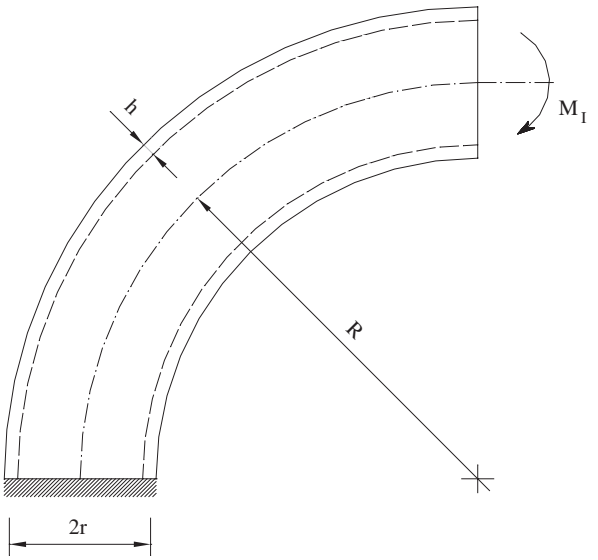

Fig. 3 Cylindrical pipe under in-plane moment loading

and strains than those present in a straight pipe of the same size and material, under the same loading conditions. For this reason pipe bends are considered as critical components of a piping system.

Consider a 90° elbow with mean radius r, bend radius of curvature R and thickness h as shown in the Fig. 3. One of its ends is assumed clamped and the other one is subjected to an in-plane closing moment M_I. The following geometrical parameters are adopted: $R = 1800\,\text{mm}$, $r = 300\,\text{mm}$, $h = 15\,\text{mm}$. In this example, only the moment M_I and the yield stress σ_y are considered as random variables with mean values μ_s, μ_r and standard deviations σ_s, σ_r respectively.

5.1.1 Limit Load Analysis

From the deterministic analysis, we got the limit moment as $0.4614 \times 4hr^2\sigma_y$. The limit state function is a linear function of basic variables X, Y and defined by

$$g(X, Y) = 0.4614 \times 4hr^2 Y - X. \tag{35}$$

Staat and Heitzer [18] introduced the analytical expressions of the reliability indices for both cases of normally and log-normally distributed random variables, respectively

$$\beta_{HL} = \frac{0.4614 \times 4hr^2\mu_r - \mu_s}{\sqrt{\left(0.4614 \times 4hr^2\right)^2 \sigma_r^2 + \sigma_s^2}}, \tag{36}$$

$$\beta_{HL} = \frac{\log\left(0.4614 \times 4hr^2 m_r\right) - \log\left(m_s\right)}{\sqrt{\delta_r^2 + \delta_s^2}}, \tag{37}$$

where m_r, m_s and δ_r, δ_s are calculated as

$$m_{r,s} = \mu_{r,s} e^{-\delta_{r,s}^2/2} = \frac{\mu_{r,s}}{\sqrt{\left(\frac{\sigma_{r,s}^2}{\mu_{r,s}^2} + 1\right)}}, \quad \delta_{r,s} = \sqrt{\log\left(\frac{\sigma_{r,s}^2}{\mu_{r,s}^2} + 1\right)}. \tag{38}$$

5.1.2 Shakedown Load Analysis

For this case the in-plane bending moment M_I varies within the range $[-M_0, M_0]$ and only the amplitudes but not the uncertain complete load history influence the solution. Consider the case where the value M_0 is a random variable. From the deterministic analysis, we got the shakedown limit as $0.2507 \times 4hr^2\sigma_y$. The limit state function is a linear function of basic variables X, Y and defined by

$$g(X, Y) = 0.2507 \times 4hr^2 Y - X, \tag{39}$$

and the reliability indices for both cases of normally and log-normally distributed random variables are obtained, respectively

$$\beta_{HL} = \frac{0.2507 \times 4hr^2\mu_r - \mu_s}{\sqrt{\left(0.2507 \times 4hr^2\right)^2 \sigma_r^2 + \sigma_s^2}}, \tag{40}$$

$$\beta_{HL} = \frac{\log\left(0.2507 \times 4hr^2 m_r\right) - \log\left(m_s\right)}{\sqrt{\delta_r^2 + \delta_s^2}}. \tag{41}$$

The failure probabilities P_f are presented in Figs. 4 and 5 versus $\mu_s/4hr^2\mu_r$. Numerical solutions of the limit and shakedown analyses are compared with the analytical ones resulting from exact solutions. For each case, both random variables are normally or log-normally distributed with standard deviations $\sigma_{r,s} = 0.1\mu_{r,s}$. It is shown that our results correspond well with the analytical ones for all cases.

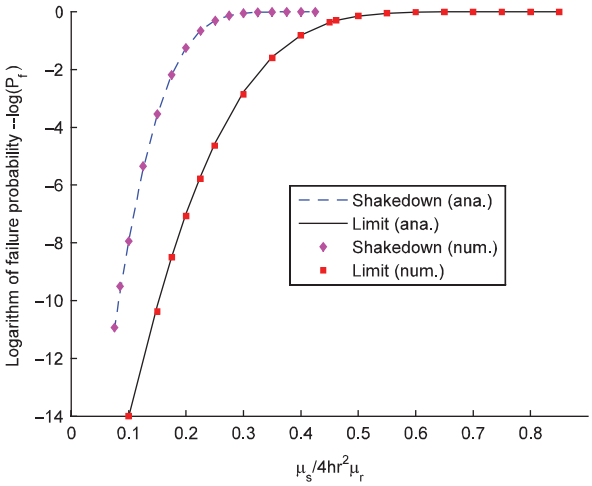

Fig. 4 Comparison of the results for normally distributed variables

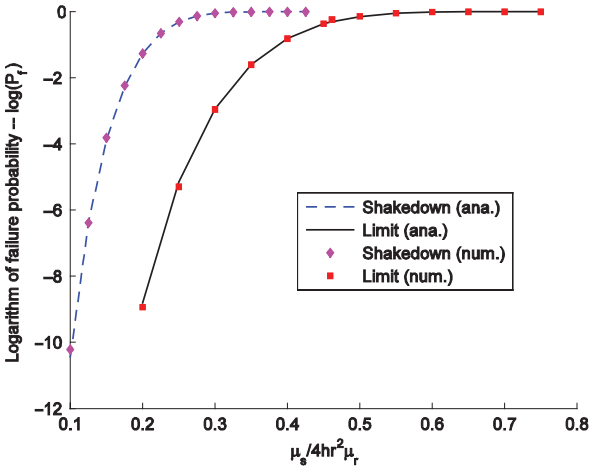

Fig. 5 Comparison of the results for log-normally distributed variables

5.2 Limit Analysis of Cylindrical Pipe Under Complex Loading

Beside the loading and material strength, it is well known that the load carrying capacity of shell structures is generally influenced by their initial imperfections which occur during the manufacturing and construction stages such as variability of thickness. In this example, the effect of thickness imperfection on the limit loads of a shell structure is examined. The cylindrical

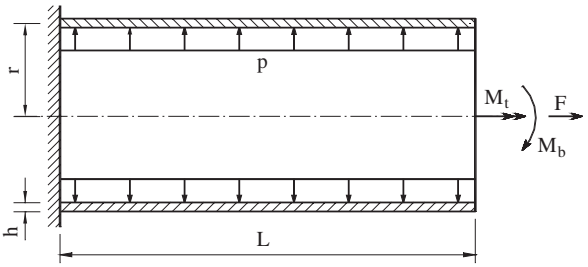

Fig. 6 Cylindrical pipe under complex loading

pipe subjected to complex loading is considered here, see Fig. 6. The following geometrical and physical parameters are adopted: $L = 2700\,\text{mm}$, $r = 300\,\text{mm}$, $\sigma_y = 120\text{MPa}$. For this purpose, only the loading and the thickness h of the pipe are modeled as random variables. Four loading cases are examined.

5.2.1 Internal Pressure

For this case, the exact plastic collapse limit pressure is given by $p_{\text{lim}} = \sigma_y h/r$. Thus, the resistance R depends linearly on the realization h of the thickness basic variable Z. The magnitude of the internal pressure is the second basic variable X. The limit state function is defined by

$$g(X, Z) = \frac{\sigma_y}{r} Z - X. \tag{42}$$

If both thickness and load random variables are supposed to be normally distributed with mean values μ_t, μ_s and standard deviations σ_t, σ_s respectively, then the limit state function $g(\mathbf{U})$ in the standard Gaussian space is a linear function. Note that σ_y is the yield stress and not a standard deviation here. The mean and standard deviation of the limit state function can be calculated as follows

$$\mu_g = \frac{\sigma_y}{r}\mu_t - \mu_s, \quad \sigma_g = \sqrt{\left(\frac{\sigma_y}{r}\right)^2 \sigma_t^2 + \sigma_s^2}, \tag{43}$$

from which, the reliability index becomes

$$\beta_{HL} = \frac{\mu_g}{\sigma_g} = \frac{\left(\frac{\sigma_y}{r}\right)\mu_t - \mu_s}{\sqrt{\left(\frac{\sigma_y}{r}\right)^2 \sigma_t^2 + \sigma_s^2}}. \tag{44}$$

The limit state function becomes nonlinear if both basic variables are lognormally distributed. Analogously to (44), we obtain the exact reliability index for FORM

$$\beta_{HL} = \frac{\log\left(\left(\frac{\sigma_y}{r}\right) m_t\right) - \log\left(m_s\right)}{\sqrt{\delta_t^2 + \delta_s^2}}, \tag{45}$$

where m_t, m_s and δ_t, δ_s are calculated as

$$m_{t,s} = \mu_{t,s} e^{-\delta_{t,s}^2/2} = \frac{\mu_{t,s}}{\sqrt{\left(\frac{\sigma_{t,s}^2}{\mu_{t,s}^2} + 1\right)}}, \quad \delta_{t,s} = \sqrt{\log\left(\frac{\sigma_{t,s}^2}{\mu_{t,s}^2} + 1\right)}. \tag{46}$$

5.2.2 Bending Moment

The exact plastic collapse limit moment is linearized by $M_b^{\lim} = 4r^2\sigma_y h$. The limit state function is a linear function of basic variables X, Z and defined by

$$g(X, Z) = 4r^2\sigma_y Z - X. \tag{47}$$

The reliability indices for both cases of normally and log-normally distributed random variables are obtained, respectively

$$\beta_{HL} = \frac{4r^2\sigma_y\mu_t - \mu_s}{\sqrt{\left(4r^2\sigma_y\right)^2\sigma_t^2 + \sigma_s^2}}, \tag{48}$$

$$\beta_{HL} = \frac{\log\left(4r^2\sigma_y m_t\right) - \log\left(m_s\right)}{\sqrt{\delta_t^2 + \delta_s^2}}. \tag{49}$$

5.2.3 Torsion Moment

In this case the exact plastic collapse limit moment is given by $M_t^{\lim} = 2\pi r^2\sigma_y h/\sqrt{3}$. The limit state function is a linear function of basic variables X, Z and defined by

$$g(X, Z) = \frac{2}{\sqrt{3}}\pi r^2\sigma_y Z - X. \tag{50}$$

The reliability indices for both cases of normally and log-normally distributed random variables are obtained, respectively

$$\beta_{HL} = \frac{\frac{2}{\sqrt{3}}\pi r^2\sigma_y\mu_t - \mu_s}{\sqrt{\left(\frac{2}{\sqrt{3}}\pi r^2\sigma_y\right)^2\sigma_t^2 + \sigma_s^2}}, \tag{51}$$

$$\beta_{HL} = \frac{\log\left(\frac{2}{\sqrt{3}}\pi r^2 \sigma_y m_t\right) - \log(m_l)}{\sqrt{\delta_t^2 + \delta_l^2}}. \tag{52}$$

5.2.4 Axial Load

The exact plastic collapse limit load is given by $F_{\lim} = 2\pi r\sigma_y h$. The limit state function is a linear function of the basic variables X, Z and defined by

$$g(X, Z) = 2\pi r\sigma_y Z - X. \tag{53}$$

The reliability indices for both cases of normally and log-normally distributed random variables are obtained, respectively

$$\beta_{HL} = \frac{2\pi r\sigma_y \mu_t - \mu_s}{\sqrt{(2\pi r\sigma_y)^2 \sigma_t^2 + \sigma_s^2}}, \tag{54}$$

$$\beta_{HL} = \frac{\log(2\pi r\sigma_y m_t) - \log(m_s)}{\sqrt{\delta_t^2 + \delta_s^2}}. \tag{55}$$

The failure probabilities P_f are presented in Figs. 7, 8, 9 and 10 with the units kN and m of force and length, respectively. The numerical solutions of the limit analyses are compared with the analytical ones resulting from exact solutions. For each loading case, both random variables are normally or log-normally distributed with standard deviations $\sigma_{t,s} = 0.1\mu_{t,s}$. It is shown that our results compare well with the analytical ones for all cases.

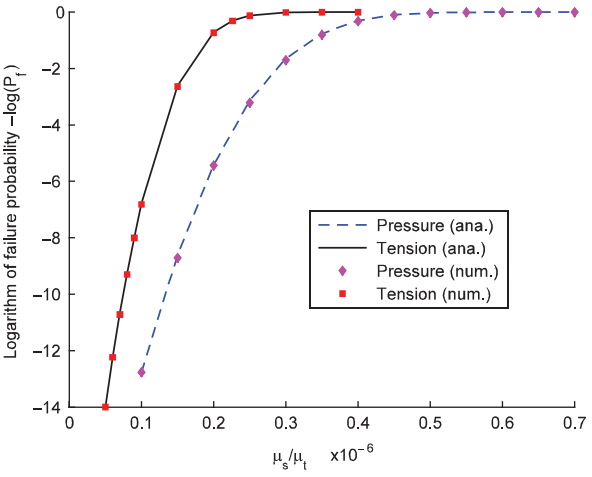

Fig. 7 Comparison of the results for normally distributed variables (kN, m)

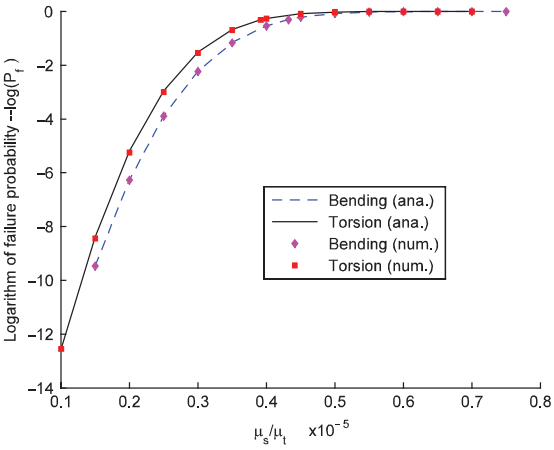

Fig. 8 Comparison of the results for normally distributed variables (kN, m)

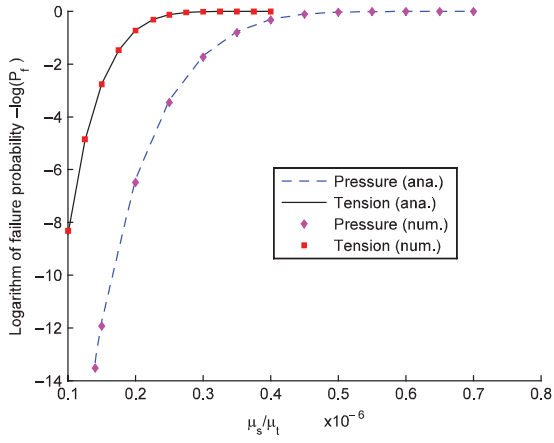

Fig. 9 Comparison of the results for log-normally distributed variables (kN, m)

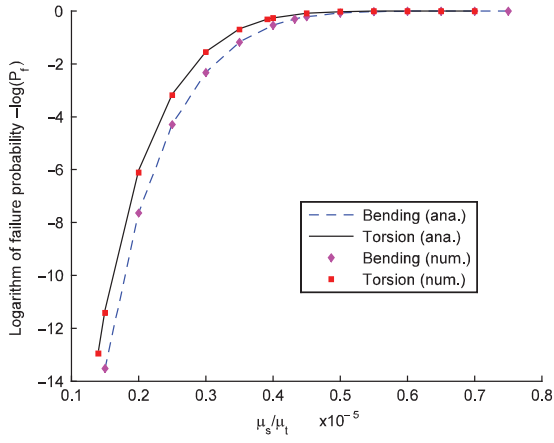

Fig. 10 Comparison of the results for log-normally distributed variables (kN, m)

6 Conclusions

A procedure for reliability analysis of inelastic shell structures under variable loads which is based on a direct plasticity method has been presented. The procedure involves a deterministic limit and shakedown analysis for each probabilistic iteration. The loading and strength of the material as well as the thickness of the shell are considered as random variables. The proposed method appears to be capable of identifying good estimates of the failure probability for the most probable failure mode, even in the case of very small probabilities. The possible extension to multiple failure modes is indicated. The proposed method makes the analysis problem of any load history time-invariant and it is applicable with incomplete data. Sensitivity analyses are obtained directly from a mathematical optimization with no extra computational cost.

Acknowledgements The work of Thanh Ngọc Trần has been supported by the Deutscher Akademischer Austauschdienst (DAAD). The work of Phú Tình Phạm has been supported by the Ministry of Education and Training of Vietnam (MOET) through the 322 project. The work of Đức Khôi Vũ has been supported by the A. von Humboldt Foundation. The authors thank the reviewer for some stimulating comments.

References

1. Alibrandi, U., Ricciardi, G. (2008) The use of stochastic stresses in the static approach of probabilistic limit analysis. Int. J. Numer. Meth. Engng 73(6), 747–782. doi:10.1002/nme.2089
2. Augusti, G., Baratta, A., Casciati, F. (1984) Probabilistic methods in structural engineering. Chapman and Hall, London.
3. Burgoyne, C.J., Brennan, M.G. (1993) Exact Ilyushin yield surface. Int. J. Sol. Struct. 30(8), 1113–1131. doi:10.1016/0020-7683(93)90007-T
4. Caddemi, S., Ricciardi, G., Saccà, C. (2002) Limit analysis of structures with stochastic strengths by a static approach. Meccanica 37(6), 527–544. doi:10.1023/A:1020939103140
5. Capsoni, A., Corradi, L. (1997) A finite element formulation of the rigid-plastic limit analysis problem. Int. J. Num. Meth. Engng 40(11), 2063–2086. doi:10.1002/(SICI)1097-0207(19970615) 40:11<2063::AID-NME159>3.0.CO;2-%23
6. Code_Aster 7.3 (2003) User's manual. A product of EDF R&D, Clamart, France. http://www.code-aster.org
7. Der Kiureghian A., Dakessian T. (1998) Multiple design points in first and second-order reliability. Struct. Saf, 20(1), 37–49. doi:10.1016/S0167-4730(97)00026-X
8. European Standard (2005–06) Unfired pressure vessels – Part 3: Design, Annex 2: Annex B Direct route for design by analysis, CEN European Committee for Standardization, EN 13445-3:2002, Issue 14
9. GiD 7.2 (2002) User's manual. A product of the Center for Numerical Methods in Engineering (CIMNE), Barcelona. http://www.gid.cimne.upc.es
10. Gollwitzer, S., Abdo, T., Rackwitz, R. (1988) FORM Manual. RCP GmbH, München.
11. Hasofer, A.M., Lind, N.C. (1974) An exact and invariant first order reliability format. ASCE, J. Eng. Mech. Div. 100, No. EM1, 111–121

12. Heitzer, M., Staat, M. (2000) Reliability analysis of elasto-plastic structures under variable loads. In: Maier, G., Weichert, D. (eds.) Inelastic analysis of structures under variable loads: Theory and engineering Applications. Kluwer, Academic Press, Dordrecht, 269–288
13. Heitzer, M., Staat, M. (2002) Limit and shakedown analysis with uncertain data. In: Marti, K. (ed.) Stochastic optimization techniques, numerical methods and technical applications. Springer, Heidelberg, 253–267
14. Ilyushin, A.A. (1948) Plasticity. Moscow: Gostekhizdat, In Russian
15. Klingmüller, O. (1979) Anwendung der Traglastberechnung für die Beurteilung der Sicherheit von Konstruktionen. Dissertation, Universität Essen Gesamthochschule
16. Madsen, H.O., Krenk, S., Lind, N.C. (1986) Methods of structural safety. Prentice-Hall, Englewood Cliffs, NJ
17. Seitzberger, M. (2000) Contributions to an efficient numerical analysis of the plastic behaviour of thin-walled structures. Fortschritt-Berichte VDI, Reihe 18, Nr. 247, VDI-Verlag, Düsseldorf
18. Staat, M., Heitzer, M. (2003) Probabilistic limit and shakedown problems. In: Staat, M., Heitzer, M. (eds.) Numerical methods for limit and shakedown analysis. Deterministic and probabilistic problems. NIC Series Vol. 15, John von Neumann Institute for Computing, Jülich, 217–268. http://www.fz-juelich.de/nic-series/volume15/nic-series-band15.pdf
19. Trần, T.N., Kreißig, R., Vu, D.K., Staat, M. (2007) Upper bound limit and shakedown analysis of thin shells using the exact Ilyushin yield surface. Comput. Struct., 86(17–18) 1683–1695. doi:10.1016/j.compstruc.2008.02.005
20. Trần, T.N., Kreißig, R., Staat, M. (2008) Probabilistic limit and shakedown analysis of thin shells using the exact Ilyushin yield surface. Struct. Saf. doi:10.1016/j.strusafe.2007.10.003
21. Trần, T.N. (2008) Limit and shakedown analysis of plates and shells including uncertainties. Dissertation, TU Chemnitz. http://archiv.tu-chemnitz.de/pub/2008/0025
22. Tvedt, L. (1983) Two second-order approximations to the failure probability. Veritas Report RDIV/20-004-83, Det Norske Veritas, Oslo, Norway